ACS chemical biology

Articles

pubs.acs.org/acschemicalbiology

Deciphering Structural Elements of Mucin Glycoprotein Recognition

Andrew Borgert,[†,#] Jamie Heimburg-Molinaro,[‡,#] Xuezheng Song,[‡] Yi Lasanajak,[‡] Tongzhong Ju,[‡] Mian Liu,[§] Pamela Thompson,[§] Govind Ragupathi,[∥] George Barany,[⊥] David F. Smith,[‡] Richard D. Cummings,*[,‡] and David Live*[,§]

[†]Center for Magnetic Resonance Research and [⊥]Department of Chemistry, University of Minnesota, Minneapolis, Minnesota 55455, United States

[‡]Department of Biochemistry, Emory University, Atlanta, Georgia 30322, United States

[§]Complex Carbohydrate Research Center, University of Georgia, Athens, Georgia 30602, United States

[∥]Memorial Sloan-Kettering Cancer Center, New York, New York 10065, United States

Supporting Information

ABSTRACT: Mucin glycoproteins present a complex structural landscape arising from the multiplicity of glycosylation patterns afforded by their numerous serine and threonine glycosylation sites, often in clusters, and with variations in respective glycans. To explore the structural complexities in such glycoconjugates, we used NMR to systematically analyze the conformational effects of glycosylation density within a cluster of sites. This allows correlation with molecular recognition through analysis of interactions between these and other glycopeptides, with antibodies, lectins, and sera, using a glycopeptide microarray. Selective antibody interactions with discrete conformational elements, reflecting aspects of the peptide and disposition of GalNAc residues, are observed. Our results help bridge the gap between conformational properties and molecular recognition of these molecules, with implications for their physiological roles. Features of the native mucin motifs impact their relative immunogenicity and are accurately encoded in the antibody binding site, with the conformational integrity being preserved in isolated glycopeptides, as reflected in the antibody binding profile to array components.

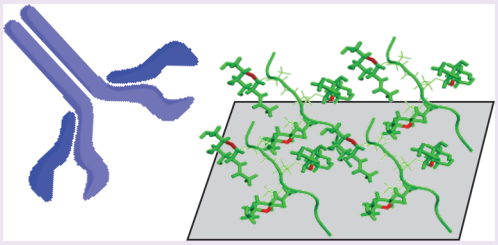

The number of glycan structures of the human glycome is estimated to be many thousands.[1] This diversity, arising from the variety of residues and multiple linkage options, is also amplified by glycan conjugation to other components including proteins and lipids. A large fraction of mammalian proteins are glycosylated,[2] and the combinatorial possibilities of these glycoconjugates present a complexity unparalleled in genomics and proteomics, further compounded by the intrinsic heterogeneity in glycoproteins, thought to be a consequence of nontemplate driven glycosylation. Additionally, cellular regulation of glycan structures and patterns through differential enzyme expression in the normal or disease states allows cell surface glycoproteins to function as temporally regulated biomarkers. The endogenous presentation of aberrant glycosylation can also give rise to circulating antibodies that serve as secondary markers.[3] Given their prominence in communication between cells and surroundings, understanding the contributions made by the protein and glycan components to molecular recognition are critical in how information is encoded for specific glycoprotein interactions and functions.

Mucin-type *O*-glycosylation, characterized by a prevalence of threonine and serine residues modified with *N*-acetylgalactosamine (GalNAc), constitutes a major and complex form of protein modification, encountered on the cell surface. Mucin *O*-glycan biosynthesis occurs in a stepwise fashion, initiated by members of a family of about two dozen polypeptide *N*-acetylgalactosaminyltransferases (ppGalNAcTs),[4] followed by elaboration with other sugars to generate complex *O*-glycans. The glycosylation patterns generated by these enzymes are conferred by the catalytic domains[5] and, if proximal *O*-GalNAcs are already in place, influenced by their lectin domains.[6,7] However, the lack of strictly defined consensus sequences for *O*-glycosylation,[5] together with the known heterogeneity in *O*-glycan structures, creates challenges for defining discrete mucin recognition elements.

Characterization of *O*-glycosylation by mass spectral methods typically relies on chemically released glycans, with loss of crucial sequence-specific data on sites of modification. Non-destructive analysis with lectins of known carbohydrate epitope preferences is also commonly used,[8] but lectins are largely insensitive to the glycoconjugate context. Their apparent affinities may reflect the degree to which pendant glycans are clustered, providing some basis for selectivity, but this can be rationalized in global thermodynamic terms without a detailed structural knowledge.[9] These analytical limitations have given rise to an intrinsic ambiguity in defining the *O*-glycan epitopes. For instance, serine/threonine α-*O*-GalNAc is referred to as the

Received: December 15, 2011
Accepted: March 23, 2012
Published: March 23, 2012

Tn antigen, not discriminating the amino acid to which it is attached,[10] providing insufficient definition of this epitope in the context of a glycoprotein. This structure, which is normally rare in humans, is relevant because of the correlation of its aberrant appearance with poor prognosis in cancer, where altered densities and clustering are observed.[11−13] It has been a target in diagnostic and therapeutic strategies, particularly in development of glycoconjugate antitumor vaccines.[12,14] Understanding the conformation of mucins even with the minimal Tn antigen is broadly relevant to mucin structural biology since the α-*O*-GalNAc residue of their glycans is key in organizing the core glycoprotein scaffold[15] underlying potentially more complex pendant glycans.

The relevance of more accurate characterization of epitopes with S/T-α-*O*-GalNAc is indicated by the differential recognition of glycosylation in isolated sites or in clusters by antibodies in normal immune responses and those induced in therapeutic applications of glycoconjugate vaccines.[3,12,16] Results from surface plasmon resonance[17] and array binding studies[3,18,19] show that antibody recognition of mucin structures is influenced by presentation in the glycoconjugate environment, but these findings have not been accompanied by any structural studies. The importance of this is illustrated in a recent crystal structure of a T-α-*O*-GalNAc glycopeptide−antibody complex showing contacts between the antibody and both carbohydrate and peptide portions.[20] Since material isolated from natural sources displays microheterogeneity even if isolated from a single cell type, we have employed chemical synthesis to provide homogeneous well-defined material needed for biophysical studies using NMR methods for a systematic analysis of mucin conformation as a function of glycosylation density. The constructs examined in this way and others have been assembled in a glycopeptide microarray to gain further insight into how conformational properties mediate binding of lectins and antibodies.

RESULTS AND DISCUSSION

Structural Analysis of Mucin Glycopeptides. The conformations of several glycopeptides based on the MUC2 related peptide sequence PTTTPLK, Ac-PTTTPLK-NH_2 (PEP), Ac-PT*TTPLK-NH_2 (A), Ac-PTT*TPLK-NH_2 (B), Ac-PTTT*PLK-NH_2 (C), Ac-PT*T*TPLK-NH_2 (D), Ac-PT*TT*PLK-NH_2 (E), Ac-PTT*T*PLK-NH_2 (F), and Ac-PT*T*T*PLK-NH_2 (G), where * indicates modification with α-*O*-GalNAc, were studied by NMR methods. These allow examination of incremental effects of glycosylation and were previously biochemically characterized as ppGalNAcT substrates,[21] showing differential reactivity. Their syntheses and preliminary NMR have been reported.[22] More extensive NMR data, including NOEs and vicinal couplings, have now been obtained and were used in the structure determination. Relationships to the features of other mucin motifs based on initial models were noted.[23] The backbone $^3J_{HN-H\alpha}$ and threonine side-chain $^3J_{H\alpha-H\beta}$ values measured (Table 1, Supporting Information Figure 1) are correlated with bond torsion angles.[24,25] Increasing values of the $^3J_{HN-H\alpha}$ coupling on the modified residues indicate a locally more extended arrangement and, being closer to the maximum, limit possible angular averaging for this bond. Upon glycosylation, the values of the $^3J_{H\alpha-H\beta}$ coupling associated with the respective threonine side chains are near its minimum value, indicating both limited or no averaging and an angle in the vicinity of 90° between the protons, with NOEs eliminating the other possible solution.

Orientations of GalNAc residues on a given T residue relative to the peptide backbone largely appear unaffected by the presence of neighboring glycans. This is reflected by the fact that the NOE contacts (Figure 1) between the GalNAc *N*-acetyl methyl groups and peptide backbone amides of each construct containing a single GalNAc, A, B, and C are preserved for the respective sites in the fully glycosylated G, where all three sites are occupied by GalNAc. The *N*-acetyl group orientation appears largely fixed relative to the sugar ring, indicated by the large coupling constant of ∼10 Hz between the *N*-acetyl amide proton and H2, so the NOEs provide information on the orientation of the GalNAc ring. With increasing glycosylation density there are a greater number of NOE contacts, arising from the additional protons introduced by the GalNAc residues and among those in the peptide backbone, implying an increased organization at higher levels of glycosylation. Based on experimental constraints, full structures of the glycopeptides have been computed, revealing single well-defined families of structures for each construct with coordinates and NOE constraints deposited in the Protein Data Bank (Supporting Information Figure 2 and Table 1). The closest to the average solution of the TTT segment for the amino acid and pendant GalNAc of constructs A−F are shown in Figure 2 with the trace of the peptide in the plane of the paper, each superimposed on G. The backbone traces for the full length of the glycopeptides also show a remarkable degree of similarity with the possible exception of the *N*-terminal proline residue, which is not well constrained by inter-residue experimental parameters, leaving open the possibility that this residue is mobile. The twist in the peptide backbone (Figure 2) avoids clashes between neighboring GalNAc residues and permits the orientations in the singly glycosylated forms to persist in the more densely glycosylated constructs. Relative to the axis of the peptide backbone, the GalNAc residues on adjacent threonines are oriented roughly 120° counterclockwise relative to each other (Figure 3). Further independent validation of the structures for the constructs with two or three GalNAc substitutions (D−G) was obtained through determination of residual dipolar couplings (RDC) measured for Cα**H**α, GalNAc C1H1, T methyl, T**H**β, peptide NH, and GalNAc *N*-acetyl NH in weakly aligning media.[26] When these data, which are independent of the NOE and coupling constant information, were incorporated in a further round of structure refinement of these constructs, only slight changes in the molecular geometry were found, accompanied by additional reduction in the rmsd for each family of structures. The structures of G

Table 1. Peptide Backbone and Threonine Side Chain Vicinal Coupling Constants (Hz)[a]

	construct							
	PEP	A	B	C	D	E	F	G
				$^3J_{HN-H\alpha}$				
T2	7.8	**8.8**	7.9	8.0	**8.9**	**8.6**	7.8	**8.9**
T3	8.0	8.3	**8.9**	8.1	**9.1**	8.3	**8.9**	**9.5**
T4	7.4	6.8	7.6	**8.3**	7.2	**8.0**	**8.5**	**8.5**
L6	6.6	6.3	6.3	5.9	6.1	5.7	5.5	5.5
K7	7.2	7.3	7.3	6.7	7.2	6.7	7.3	7.0
				$^3J_{H\alpha-H\beta}$				
T2	4.5	**2.2**	5.0	4.4	**2.6**	**2.6**	5.1	**2.4**
T3	4.4	3.7	**2.0**[b]	5.1	<**2.0**[c]	4.2	**ND**	**ND**
T4	6.2	5.9	5.7	**2.2**	6.1	<**2.0**[c]	**2.2**	<**2.0**[c]

[a]Glycosylated sites in bold, determined to better than ±0.2 Hz. ND, not determined. [b]Coupling only partially resolved. [c]Coupling not resolved.

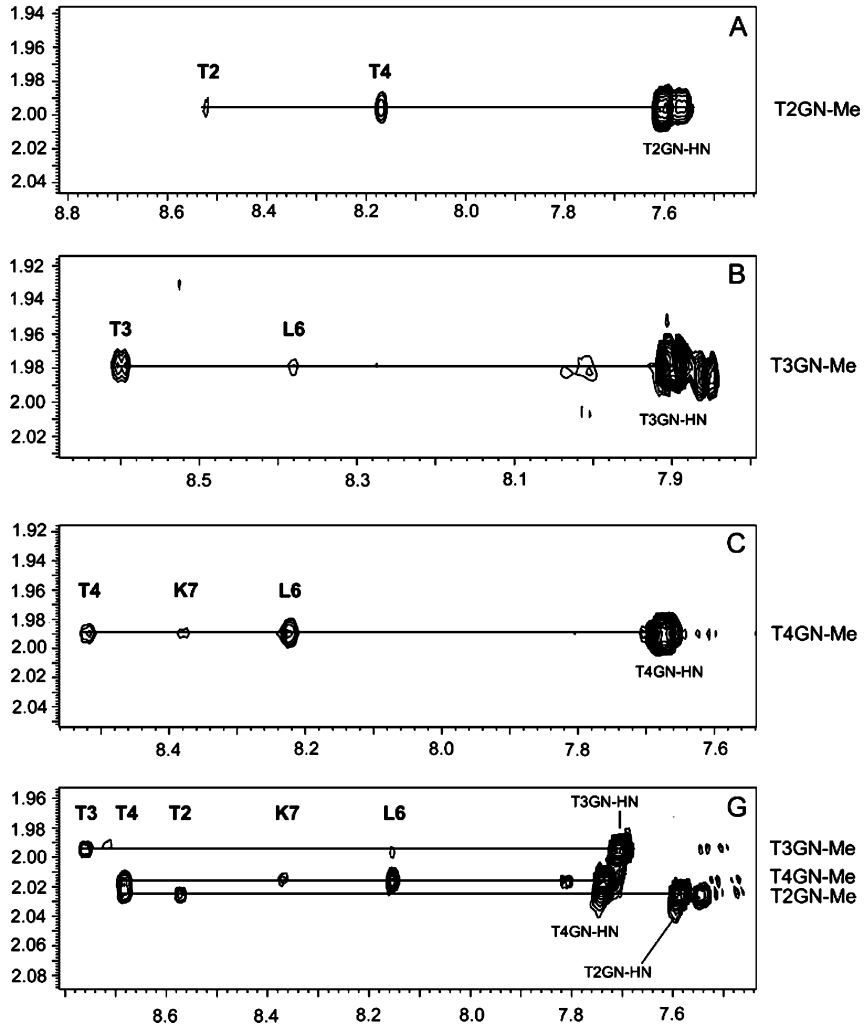

Figure 1. NOE contacts between GalNAc methyl protons and amide backbone and *N*-acetyl amide protons for the individually glycosylated forms, A, B, and C, and for the triglycosylated construct G of the PTTTPLK sequence.

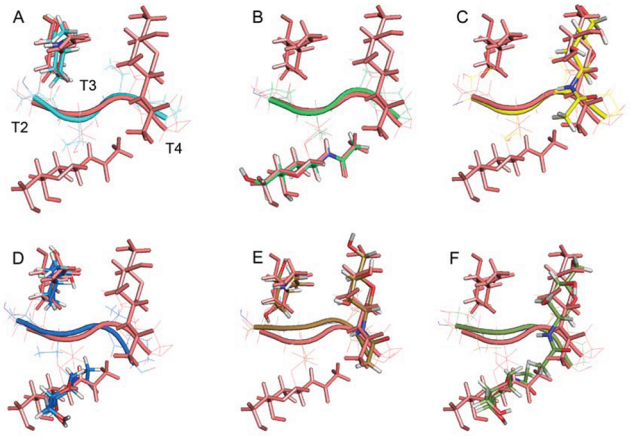

Figure 2. Closest to the average structures of the TTTP segment for the mono- and diglycosylated PTTTPLK constructs A–F, in various colors, superimposed on the structure of the triglycosylated form G (salmon); rmsd's to G for threonine and GalNAc residues heavy atoms are from A, 0.947 Å; B, 0.740 Å; C, 1.05 Å; D, 1.323 Å; E, 0.961 Å; and F, 1.447 Å. Direction of peptide backbone parallel to page. See Supporting Information Table 1 for structure statistics and PDB IDs.

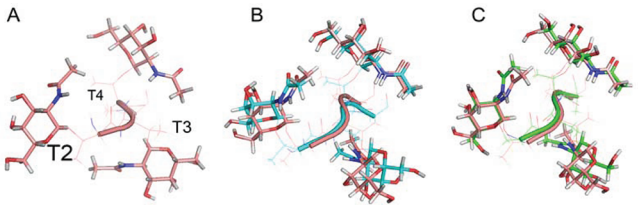

Figure 3. View down the peptide backbone (N to C, perpendicular to page) (A) for the T*T*T* segment of the G construct. (B) Superposition of the closest to the average of threonine and GalNAc heavy atoms for construct G with RDC refinement (cyan) and without RDC refinement (salmon). The rmsd between the structures is 1.194 Å. (C) Superposition of threonine and GalNAc heavy atoms of G (salmon) with the serine, threonine, and GalNAc heavy atoms of the S*T*T*T*AV structure (green) reported earlier;[15] rmsd = 1.665 Å.

before and after RDC refinement are shown in Figure 3B. Since the impact of motional averaging on the RDCs is different from that for NOEs, the consistent results reinforce the validity of a single conformational model rather than possible interconversion between multiple conformers, implying that the respective structures are quite energetically favorable and can be expected to maintain their conformational integrity when coupled to the array matrix. The conformations of the individual glycosylated amino acid residues, taken by themselves, are very similar. The results here show how the individual components assemble into

dx.doi.org/10.1021/cb300076s | *ACS Chem. Biol.* 2012, 7, 1031–1039

clusters, an arrangement found in mucins. Interestingly, aligning the peptide Cα atoms for construct A in this work and the respective atoms of the glycopeptide extracted from the recent antibody-bound glycopeptide crystal structure,[20] with the glycosylated T residues on each molecule in register, reveals very similar peptide backbone traces for each, with an rmsd of 0.655 Å between the respective Cαs. Orientation of the GalNAc relative to the peptide chain is also similar in both cases, with a difference of ~30° relative to the backbones of the Cα aligned structures. While the *O*-GalNAc modification is near the N-terminus in both cases, the sequences PT*TTPLK of A and GT*KPPL in the antibody complex are somewhat different. Qualitatively, results on a clustered Tn-glycophorin fragment are similar to our findings.[27] The NMR structure of a MUC1 single repeat glycopeptide, modified on the T of the GVTSA segment, shows NMR and conformational features quite similar to those for the individual glycosylated amino acids reported here;[28] however, it is difficult to make quantitative comparison with these or other reported NMR structures of MUC5AC[29] and other mucin models because coordinates are not available in structure databases.

Incremental glycosylation imparts enhanced rigidity to the motif as the number of both hydrogen bonding-like interactions between the GalNAc and the peptide backbone, and hydrophobic interactions between the methyl group on the GalNAc and amino acid side chains increase, similar to other systems.[15] The arrangement of the GalNAc *N*-acetyl NH group and the carbonyl of its associated amino acid is consistent with intramolecular hydrogen bonding geometries[15,30] as found in the Cambridge Data Base.[31] The same underlying organizational influences appear operative for construct G and the clustered triplet glycosylated motif solved earlier for the sequence S*T*T*AV,[15] despite the difference of contexts in which these clusters appear (Figure 3C), and support the contention of a consistent triplet cluster mucin motif. The profile of inhibition by several Tn bearing structures on the binding of sera from mice and primates, after challenge with a vaccine based on such a cluster, S*T*T*, supports this in a biological context.[32] A similar target has also been identified for the monoclonal antibody MLS128 that can inhibit cancer cell growth.[33] The determination of the structures here at atomic resolution and their stability are consistent with the extended organization of mucins.[15] This precludes contributions from sequentially remote segments in the native environment, supporting the notion that the glycopeptides offer a faithful representation of their conformations in the larger mucin glycoprotein context. With the additional information developed here on mucin scaffolds, we turned to evaluating how these features are reflected in their molecular recognition using a microarray platform populated with those glycopeptides examined here by NMR, as well as others.

Microarray Analyses. Glycan microarrays, such as implemented by the Consortium for Functional Glycomics, have emerged as a key technology for efficient screening of carbohydrate−protein interactions.[34−36] The slide-based format is attractive, requiring only minute amounts of ligand and binding proteins while providing rapid identification of carbohydrate−protein interactions. In extending this to glycoconjugate structures, arrays based on neoglycoproteins offer approximations of the local density and clustering of glycans found in mucins[35,37,38] and may be chemically more accessible but are unlikely to be completely faithful in representing the organization of mucin motifs *in vivo*.

Deviations from these native chemical structures perturb the organization[15] and recognition by antibodies,[32] particularly for clustered glycosylation. Arrays based on native mucin glycopeptide motifs, implemented here and also by others,[3,19] with direct ligation to the slide substrate or through a carrier protein,[39,40] offer more natural targets for binding studies. For the most part, in previous studies with Tn glycopeptides immobilized in a slide- or bead-based array format, the Tn epitope has only been presented in isolated sites or in pairs in the MUC1 repeat sequence,[3,18,19] with the aspect of clustering largely overlooked.

A microarray of glycopeptides with α-*O*-GalNAc S or T residues was assembled, Table 2, either clustered or in isolation. Included were those whose conformational properties and stability we have characterized in detail, described above (IDs 1−8). Additional biologically relevant glycopeptides with S/T-α-*O*-GalNAc in a variety of peptide contexts are present. These included a sequence from α-dystroglycan (IDs 9, 13), a MUC5AC sequence (ID 10),[7] a fragment of rat submandibular mucin (EA2) (IDs 11, 12) that is a known substrate for ppGalNAcTs,[41] and two segments from MUC1 (IDs 14−17). Clustered T-α-*O*-GalNAc without adjacent proline residues were also included (IDs 18, 19), similar to a motif in the MUC2 construct G. To compare responses to those with the canonical Tn antigen, the structures Ac-T-(α-*O*-GalNAc)-NH_2-$(CH_2)_3$-NH_2)(ID 20) and S- and T-(α-*O*-GalNAc)-NH_2 or -OH were present (IDs 23−26, 45, 46). Additionally, there are glycosylated peptides from the hinge region of IgA1 in the glycopeptide array (IDs 27−44).[42] Control glycans were also included (IDs 47−52).

Presence and accessibility of the Tn-bearing structures on the array was established by binding of the lectins *Helix pomatia* agglutinin (HPA) and *Vicia villosa* agglutinin (VVA), which have broad specificity for the α-GalNAc structure.[8] Representative responses for HPA and VVA at 1 μg/mL are plotted together in Figure 4A. HPA binding was consistent with the presence of α-GalNAc on the glycopeptides,[8] although those to S/T-linked α-GalNAc (IDs 23−26) and IgA-Pep03 (ID 29) were weak. VVA binding was also consistent with the presence of α-GalNAc on the printed glycoconjugates, although apparently more selective than HPA. The crystal structures of HPA and VVA in complex with S-α-*O*-GalNAc[43,44] show shallow binding pockets that interact with the exposed GalNAc hydrophilic surface. This is consistent with their broad specificity and general use for detecting GalNAc.

The array was further interrogated with a panel of seven anti-Tn monoclonal IgM antibodies (mAbs) from the laboratory of Georg Springer,[45,46] elicited from mice by Tn-bearing red blood cells and Tn components derived from O-type red blood cells.[46] The seven mAbs were grouped into three subsets, BaGs 1−4, BaGs 5 and 6, and BaGs 7, based on the pattern of glycosylated structures recognized (Figure 4B−D). The mAbs show little preference for glycopeptides when the T-α-*O*-GalNAc (the canonical Tn structure) is presented at an isolated site of glycosylation, while strongly preferring adjacent pairs or triplets, but interestingly not a sequence of four T-α-*O*-GalNAc sites.

For the series of MUC2 glycopeptides (IDs 1−7) studied by NMR, antibodies BaGs 1−4 only recognize monoglycosylated species when the GalNAc is on T2, but not on T3 or T4, despite the similarity of the conformation of the individual glycosylated amino acids. They recognize all three of the diglycosylated species and the fully glycosylated cluster, as well as, more weakly, an isolated triplet of three T-α-*O*-GalNAc (Tn_3) residues on a linker. The other singly or multiply glycosylated constructs in different contexts from MUC1, MUC5AC,

Table 2. Structures on Glycopeptide Array[a]

chart ID	detail	sequence
1	A-MUC2	AcPT*TTPLK-NH_2
2	B-MUC2	AcPTT*TPLK-NH_2
3	C-MUC2	AcPTTT*PLK-NH_2
4	D-MUC2	AcPT*T*TPLK-NH_2
5	E-MUC2	AcPT*TT*PLK-NH_2
6	F-MUC2	AcPTT*T*PLK-NH_2
7	G-MUC2	AcPT*T*T*PLK-NH_2
8	R-MUC2	AcPTTTPLK-NH_2
9	α-Dystroglycan	AcPPTTTTKKP-NH_2
10	MUC5AC	H_2N-GTTPSPVPT*TSTTSAP-OH
11	EA2	AcPTTDSTT*PAPTTKNH_2
12	EA2-R	AcPTTDSTTPAPTTKNH_2
13	α-Dystroglycan	AcPPT*T*T*T*KKP-NH_2
14	MUC1−1	NH_2-TSAPDT*RDAP-NH_2
15	MUC1−1R	NH_2-TSAPDTRDAP-NH_2
16	MUC1−2	H_2N-APGS*T*APP-NH_2
17	MUC1−2R	H_2N-APGSTAPP-NH_2
18	PADRE Tn3[b]	H_2N-GaKcVAAWTLKAAaT*T*T*GCONH_2
19	Tn3 linker	Ac-T*T*T*-NH$(CH_2)_3NH_2$
20	Tn linker	Ac-T*-NH$(CH_2)_3NH_2$
21	Peptide-4	H_2N-KTTT-CONH_2
22	Peptide-5	H_2N-KTTTG-CONH_2
23	Ser-GalNAc1	H_2N-Ser(α-D-GalNAc)-NH_2
24	Ser-GalNAc2	H_2N-Ser(α-D-GalNAc)-OH
25	Thr-GalNAc1	H_2N-Thr(α-D-GalNAc)-NH_2
26	Thr-GalNAc2	H_2N-Thr(α-D-GalNAc)-OH
27	IgA-Pep01	H_2N-KPVPST*PPT*PS*C-OH
28	IgA-Pep02	H_2N-KPVPSTPPTPSC-OH
29	IgA-Pep03	H_2N-KPVPS*TPPTPSC-OH
30	IgA-Pep04	H_2N-KPST*PPT*PS*PS*C-OH
31	IgA-Pep05	H_2N-KPSTPPTPSPSC-OH
32	IgA-Pep06	H_2N-KT*PPT*PS*PS*TPC-OH
33	IgA-Pep07	H_2N-KTPPTPSPSTPC-OH
34	IgA-Pep08	H_2N-KTPPTPSPST*PC-OH
35	IgA-Pep09	H_2N-KPT*PS*PS*TPPT*C-OH
36	IgA-Pep10	H_2N-KPSPSTPPTPSC-OH
37	IgA-Pep11	H_2N-KPS*PS*TPPT*PSC-OH
38	IgA-Pep12	H_2N-KPSTPPTPSPSC-OH
39	IgA-Pep13	H_2N-KPS*TPPT*PSPSC-OH
40	IgA-Pep14	H_2N-KPSTPPTPSPSC-OH
41	IgA-Pep15	H_2N-KPST*PPTPS*PS*C-OH
42	IgA-Pep16	H_2N-KPSTPPTPS*PSC-OH
43	IgA-Pep17	H_2N-KPSTPPTPSPS*C-OH
44	IgA-Pep18	H_2N-KPST*PPTPSPSC-OH
45	Ser-GalNAc-2	H_2N-Ser(α-D-GalNAc)-OH
46	Thr-GalNAc-2	H_2N-Thr(α-D-GalNAc)-OH
47	Blood group A tetra	
48	Blood group A penta	
49	LNnT	
50	Man5	
51	PBS	
52	Biotin	

[a]* = GalNAc residue on Ser or Thr. [b]For PADRE sequence a = D-Ala, c = cyclohexylalanine.

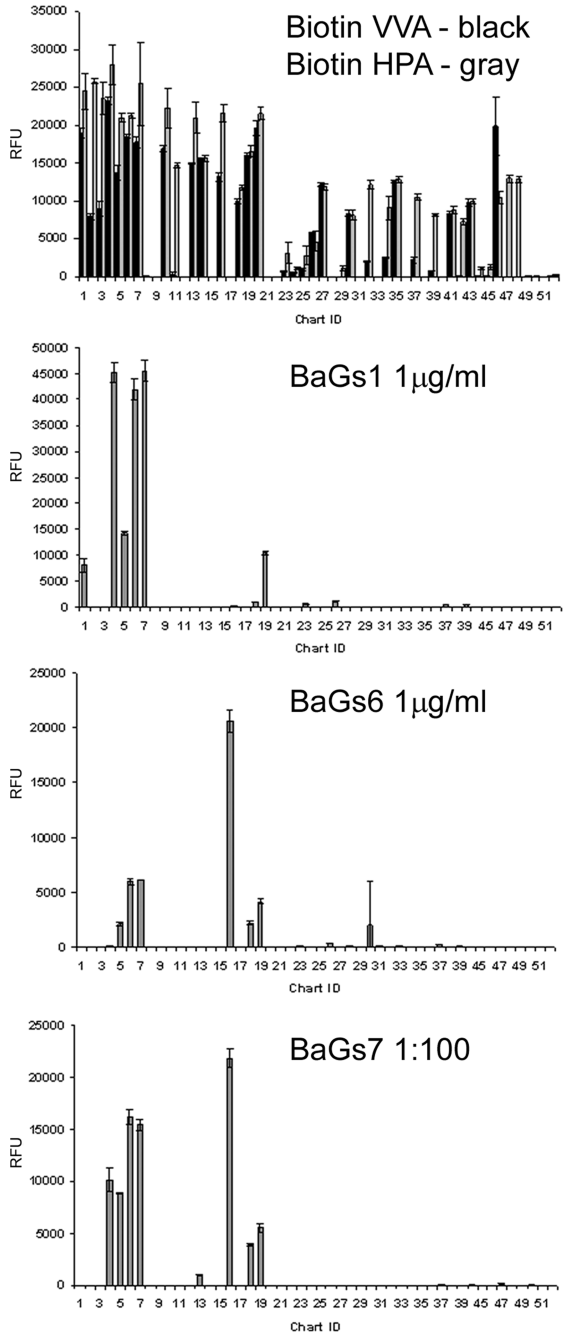

Figure 4. (A) Binding profile of biotinylated HPA lectin (gray bars) and biotinylated VVA lectin (solid black bars) both at 1 μg/mL detected with Cyanine5-labeled streptavidin. Binding profiles of (B) BaGs1 antibody representative of BaGs1, 2, 3, and 4 and (C) antibody BaGs6, representative of BaGs5 and 6 binding profiles. mAbs were assayed at 10 μg/mL detected with AlexaFluor488-labeled anti-mouse IgM (5 μg/mL). (D) Binding profile of BaGs7 antibody (1:100 dilution of ascites fluid) detected with AlexaFluor488-anti-mouse IgM (5 μg/mL). Error bars represent ±1 SD. RFU = relative fluorescence units. ID corresponds to Table 2.

EA2, and IgA are largely ignored. The preferences of BaGs5 and 6 are more restricted, favoring the glycopeptide where the C-terminal pair or all three sites are glycosylated in PTTTPLK, but more weakly interacting with the construct where both the first and last Thr are glycosylated. They also interact with an isolated Tn_3 but favor an adjacent glycosylated S*T* pair in a MUC1 (ID 16) construct. BaGs7 has a profile similar to that of BaGs5 and 6, with the subtle difference that it also interacts with the PT*T*TPLK sequence. Interestingly, the antibodies did not recognize four GalNAc residues in a row. Detailed chemical structures of the immunogens that elicited the

dx.doi.org/10.1021/cb300076s | ACS Chem. Biol. 2012, 7, 1031−1039

Springer monoclonal antibodies investigated here were not known but were clearly able to induce antibodies targeted to a rather restricted range of mucin structures that allow us to infer aspects of their nature. The ability of antibodies to discriminate subtle differences in cluster glycosylation is found in surface plasmon resonance studies reported for two other anti-Tn mAbs, arising from immunization with tumor derived material, that bind to T-α-*O*-GalNAc glycopeptides with a strict requirement for adjacent glycosylation, either as a pair or in a triplet where the recognition can be abrogated when the central residue of a triplet is an unmodified T or a proline.[17]

With a better understanding of the conformational factors relating to the organization of mucin glycopeptides, we also addressed the level to which information on mucin epitopes persists through the immune response among members of a polyclonal distribution, where we have knowledge of the chemical structures of the antigen molecules. This provided an opportunity to establish responses to variations in the glycosylation motifs on the same peptide sequence. Sera from a trial evaluating the response to immunization with α-*O*-GalNAc containing MUC1 structures, antitumor therapeutic targets, were investigated on our array. Three MUC1 constructs were used in vaccination, distinguished by different glycosylation patterns on the several available S and T sites in the repeat units. Portions of the immunogens, compounds TSAPDT*RDAP (ID 14) and APGS*T*APP (ID 16), are present on the array. For Group I sera (immunogen: GVT*S*A(PDT*RPAPGS*T*APPAHGVT*S*A)$_5$C) binding was dominated by both, with ID 14 binding greater than ID 16 even though both epitopes are contained in the vaccine (Figure 5A). Group II sera (immunogen: CHGVT*SA(PDTRPAPGS*T*APPAHGVT*SA)PDTRPA) with only the glycosylated epitopes corresponding to ID 16 present generally demonstrated binding restricted to IDs 14 and 16, with the predominant response being to ID 16 (Figure 5B). Group III sera (immunogen: CHGVT*S*A-(PDT*RPAPGS*T*APPAHGVT*S*A)PDT*RPA) generally demonstrated a restricted binding pattern, similar to Group I, with compound ID 14 much higher than ID 16 (Figure 5C). Only IgG antibodies, and not IgM from the sera were bound to the array. These IgGs show very little reactivity toward any other of the Tn-containing glycopeptides on the array. No binding of preimmune sera was evident.

All vaccine constructs had the glycosylation pattern of the second element APGS*T*APP. However, the central T residue of the first sequence TSAPDT*RDAP was glycosylated only for vaccine groups I and III. Interestingly, IgGs of sera from groups I and III favored the first sequence with the GalNAc present. In group II, the IgG response to the first sequence, with or without glycosylation, was significantly diminished, with a relatively robust response to the second fragment in glycosylated form. These results illustrate that specific glycoprotein features influence the editing, processing, and presentation of the antigen. The monodisperse selectivity of these responses implies the stability of relevant structural information that is a composite of both peptide and carbohydrate components is retained in the cellular events and is recapitulated in the short glycopeptide segments used on the array.

Sera samples from one of the groups in this trial, group I, have been previously analyzed[3] on an array that included several 60-aa MUC1 constructs (three 20 residue repeats), each with distinct glycosylation patterns. Serum antibodies preferred those including either GS*T*A or this and PDT*R, in

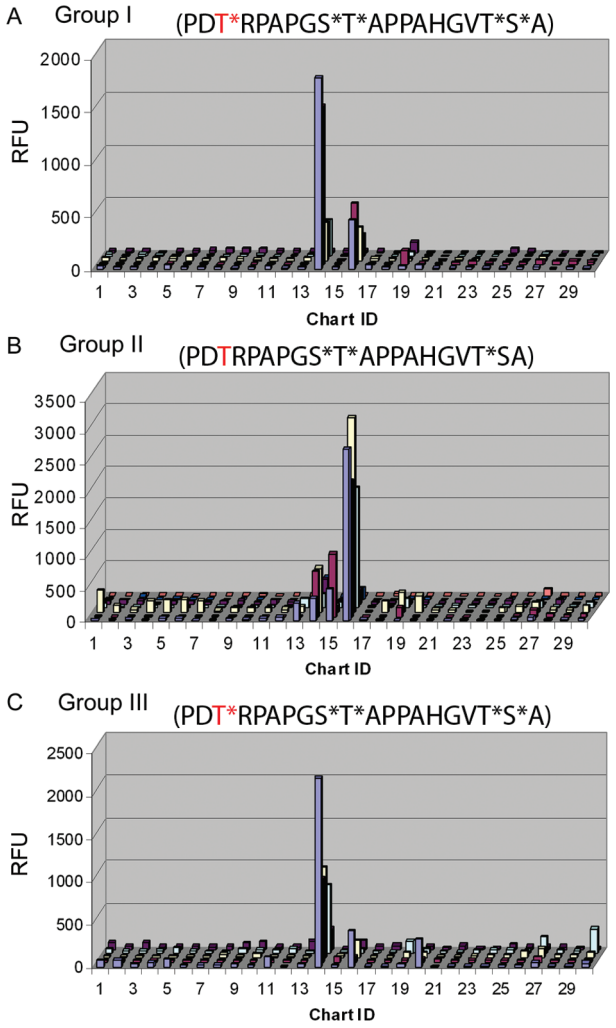

Figure 5. Binding of IgG, in RFU, in each group of sera from individuals after immunization with the respective MUC1 constructs. (A) Binding of sera from 5 individuals from Group I. (B) Binding of sera from 7 individuals from Group II. (C) Binding of sera from 5 individuals from Group III. Only results for the first 30 array components (Table 2) are shown as none of the other components indicated significant binding. Sera were diluted 1:100 and detected with AlexaFluor555-labeled anti-human IgG (5 μg/mL).

agreement with our observations for group I. When they applied group I sera to another glycopeptide array of single 20-aa repeat MUC1 glycopeptides, antibody components also recognize both epitopes.[19] These epitope preferences are further borne out by group I sera interactions with a randomized library of shorter glycopeptides.[18] Importantly here, with group II sera, we have been able to extend this analysis to show the differential impact of glycosylation on the proximal PDTRP sequence for biasing the overall response and the sensitivity of this array approach to evaluating outcomes of such vaccine therapies.

In this work, principles by which individual α-*O*-GalNAc-threonine units are assembled into larger clustered patterns of *O*-glycosylation, common in mucins, have been elucidated. Since geometries of the individual glycosylated threonines are shown to be quite similar, the selective antibody interactions observed in array screening imply the importance of relationships in the relative disposition of their glycans as presented on the multiple sites of the peptide scaffold, making up a

dx.doi.org/10.1021/cb300076s | *ACS Chem. Biol.* 2012, 7, 1031–1039

significant portion of the molecular surface, along with components of the peptide itself. Variations in glycosylation density on the same peptide sequence in which the S/T-α-*O*-GalNAc is presented can be differentiated, a factor that has not been extensively investigated before. This enhances the value of the antibodies as reagents, but full explanation of the basis for the specificity awaits additional sequence and/or structural information on the antibodies. The affinity encoded in the mAbs, raised against natural material, for the synthetic constructs we have characterized and immobilized indicates the biological relevance of the conformations. Our microarray data, as well as that of others,[3,18,19,47] affirm that, unlike lectins, antibodies broadly referred to as anti-Tn antibodies target not just the S/T-α-*O*-GalNAc structure, but surrounding features as well. They are unable to bind every potential Tn antigen site, even most presented on peptides, or the conventionally defined minimal Tn antigen. Further, the vaccination studies illustrate that in addition to ultimate antibody recognition, context and conformation play a role in mucin antigenicity, a consideration in optimal design of antimucin therapeutic agents.

METHODS

Glycopeptides. Synthesis of glycopeptides in the PTTTPLK series (ID 1−8), α-dystroglycan (ID 9 and 13), and MUC5AC (ID 10) have been reported previously.[8,22,48] The IgA derived glycopeptides were synthesized following reported procedures.[42] The MUC1 constructs (ID 14−17) and EA2 (ID 11 and 12) constructs were synthesized using standard procedures (see Supporting Information). The Tn-linker (ID 20), Tn3-linker (ID 19), and PADRE peptide Tn3 (ID 18) were provided by the laboratory of Geert-Jan Boons.

Glycopeptide Microarrays. The glycopeptide microarrays were prepared on *N*-hydroxysuccinimide (NHS) glass slides (Schott Nexterion), and immobilization of peptides and glycopeptides was achieved through amine functions. (Supporting Information) With concentrations adjusted to 100 μM in printing buffer (300 mM sodium phosphates, pH 8.5), 0.33 nL of each solution was spotted using a piezoelectric printer. The microarray was printed in spot replicates of 6. Arrays were interrogated with monoclonal anti-Tn antibodies (a kind gift from the late Georg Springer), biotinylated lectins (Vector Laboratories), and serum samples from the laboratory of Dr. Phillip Livingston at Memorial Sloan-Kettering Cancer Center (MSKCC), described below, at the given concentrations or dilutions indicated in the figures and detected with fluorescently labeled secondary antibodies and streptavidin as noted. Scanning and quantification were performed with ProScanArray scanner and ScanArray Express software (Perkin-Elmer). The list of glycans/glycopeptides printed on the microarray is given in Table 2.

NMR Analysis. NMR data were collected on Varian INOVA 600, 800, and 900 MHz instruments using pulse sequence programs in the Varian software for double-quantum filtered COSY, TOCSY, NOESY, ^{13}C and ^{15}N HSQC, and ^{13}C HMQC and HMBC experiments.[49] Samples were run at various concentrations between 2 and 10 mM in D_2O or 90% H_2O/10% D_2O. Most data were collected at 25 °C. Because of overlap in amide signals, some experiments were repeated at other temperatures in the range of 15 to 30 °C. A 300 ms mixing time was used for the NOESY experiments in 90% H_2O and 350 ms for those in D_2O. Couplings were measured from resolved peaks in 1-dimensional spectra. Structures were calculated with XPLOR-NIH[50] following the protocol described in the Supporting Information. Residual dipolar couplings were measured in didodecyl-phosphatidylcholine/dihexylphosphatidylcholine 3/1 molar ratio at 10% in 90% H_2O/10% D_2O[26] in the range of 30−35 °C using $^{1}H-^{13}C$ or $^{1}H-^{15}N$ HSQC sequences without ^{1}H decoupling pulses in the heteronuclear evolution period, and couplings were determined from splittings in the heteronuclear dimension.

Antibodies and Serum Samples. The monoclonal anti-Tn antibodies used in this study were produced by the late Georg Springer.[45,46] These mouse monoclonal IgM antibodies are designated BaGs1 (Ca3637), BaGs2 (Ca3239), BaGs3 (Ca3268), BaGs4 (Ca3342), BaGs5 (Ca3250), BaGs6 (Ca3638), and BaGs7 (Ca3749). BaGs1, 2, 3, 5, and 6 were purified by affinity chromatography, while BaGs4 and 7 were ascites fluid. Patients with breast cancer in remission were vaccinated (Supporting Information) in the adjuvant setting at MSKCC under IRB approved protocols and informed consent, with one of three Tn-MUC1-KLH (Keyhole Limpet Hemocyanin) conjugate vaccines plus immunological adjuvant QS-21.[51] The enzymatically Tn glycosylated MUC1 constructs used, prepared in the Clausen laboratory from synthetic peptides,[3,52] contained five fully glycosylated MUC1 repeats (106 aa), GVT*S*A(PDT*RPAPGS*T*APPAHGVT*S*A)$_5$C-**KLH** (Group I immunogen), 1 1/2 partially glycosylated MUC1 repeats, **KLH**-C HGVT*SA(PDTRPAPGS*T*APPAHGVT*SA)PDTRPA (Group II immunogen), or 1 1/2 fully glycosylated MUC1 repeats **KLH**-C-HGVT*S*A(PDT*RPAPGS*T*APPAHGVT*S*A)PDT*RPA (Group III immunogen).

ASSOCIATED CONTENT

Supporting Information

One-dimensional NMR spectra, overlay of families of structures for A to G, structure statisitics, RDC data, and additional methods details. This material is available free of charge via the Internet at http://pubs.acs.org.

Accession Codes

Protein Data Bank (PDB) coordinate file accession codes for MUC2 structures are A, 2LHV; B, 2LI2; C, 2LI1; D, 2LI0; E, 2LHZ; F, 2LHY; G, 2LHX and are available free of charge *via* the Internet at http://www.rcsb.org.

AUTHOR INFORMATION

Corresponding Author

*E-mail: dlive@ccrc.uga.edu; rdcummi@emory.edu.

Author Contributions

#These authors contributed equally to this work.

Notes

The authors declare the following competing financial interest(s):Dr. Ragupathi is a paid consultant and share holder in MabVax Therapeutics Inc. which has licensed the KLH-conjugate vaccines from MSKCC.

ACKNOWLEDGMENTS

This research was funded by the Georgia Research Alliance and National Institutes of Health grants RO1GM066148 and P41GM103390. We are grateful to G.-J. Boons for providing several array molecules and valuable comments and to P. Livingston for valuable discussions.

REFERENCES

(1) Cummings, R. D. (2009) The repertoire of glycan determinants in the human glycome. *Mol. Biosyst. 5*, 1087−1104.

(2) Agard, N. J., and Bertozzi, C. R. (2009) Chemical approaches to perturb, profile, and perceive glycans. *Acc. Chem. Res. 42*, 788−797.

(3) Wandall, H. H., Blixt, O., Tarp, M. A., Pedersen, J. W., Bennett, E. P., Mandel, U., Ragupathi, G., Livingston, P. O., Hollingsworth, M. A., Taylor-Papadimitriou, J., Burchell, J., and Clausen, H. (2010) Cancer biomarkers defined by autoantibody signatures to aberrant O-glycopeptide epitopes. *Cancer Res. 70*, 1306−1313.

(4) Ten Hagen, K. G., Fritz, T. A., and Tabak, L. A. (2003) All in the family: The UDP-GalNAc:polypeptide N-acetylgalactosaminyltransferases. *Glycobiology 13*, 1R−16R.

(5) Gerken, T. A., Jamison, O., Perrine, C. L., Collette, J. C., Moinova, H., Ravi, L., Markowitz, S. D., Shen, W., Patel, H., and Tabak, L. A. (2011) Emerging paradigms for the initiation of mucin-type protein O-glycosylation by the polypeptide GalNAc

transferase family of glycosyltransferases. *J. Biol. Chem. 286*, 14493−14507.
(6) Pedersen, J. W., Bennett, E. P., Schjoldager, K., Meldal, M., Holmer, A. P., Blixt, O., Clo, E., Levery, S. B., Clausen, H., and Wandall, H. H. (2011) Lectin domains of polypeptide GalNAc transferases exhibit glycopeptide binding specificity. *J. Biol. Chem. 286*, 32684−32696.
(7) Raman, J., Fritz, T. A., Gerken, T. A., Jamison, O., Live, D., Liu, M., and Tabak, L. A. (2008) The catalytic and lectin domains of UDP-GalNAc: Polypeptide alpha-N-acetylgalactosaminyltransferase function in concert to direct glycosylation site selection. *J. Biol. Chem. 283*, 22942−22951.
(8) Wu, A. M., Lisowska, E., Duk, M., and Yang, Z. G. (2009) Lectins as tools in glycoconjugate research. *Glycoconjugate J. 26*, 899−913.
(9) Dam, T. K., and Brewer, C. F. (2010) Multivalent lectin-carbohydrate interactions: Energetics and mechanisms of binding. *Adv. Carbohydr. Chem. Biochem. 63*, 139−164.
(10) Ju, T. Z., Otto, V. I., and Cummings, R. D. (2011) The Tn antigen-structural simplicity and biological complexity. *Angew. Chem., Int. Ed. 50*, 1770−1791.
(11) Desai, P. R. (2000) Immunoreactive T and Tn antigens in malignancy: Role in carcinoma diagnosis, prognosis, and immunotherapy. *Transfus. Med. Rev. 14*, 312−325.
(12) Danishefsky, S. J., and Allen, J. R. (2000) From the laboratory to the clinic: A retrospective on fully synthetic carbohydrate-based anticancer vaccines. *Angew. Chem., Int. Ed. 39*, 836−863.
(13) Slovin, S. F., Ragupathi, G., Musselli, C., Olkiewicz, K., Verbel, D., Kuduk, S. D., Schwarz, J. B., Sames, D., Danishefsky, S., Livingston, P. O., and Scher, H. I. (2003) Fully synthetic carbohydrate-based vaccines in biochemically relapsed prostate cancer: Clinical trial results with alpha-N-acetylgalactosamine-O-serine/threonine conjugate vaccine. *J. Clin. Oncol. 21*, 4292−4298.
(14) Springer, G. F. (1997) Immunoreactive T and Tn epitopes in cancer diagnosis, prognosis, and immunotherapy. *J. Mol. Med. 75*, 594−602.
(15) Coltart, D. M., Royyuru, A. K., Williams, L. J., Glunz, P. W., Sames, D., Kuduk, S. D., Schwarz, J. B., Chen, X. T., Danishefsky, S. J., and Live, D. H. (2002) Principles of mucin architecture: Structural studies on synthetic glycopeptides bearing clustered mono-, di-, tri-, and hexasaccharide glycodomains. *J. Am. Chem. Soc. 124*, 9833−9844.
(16) Kagan, E., Ragupathi, G., Yi, S. S., Reis, C. A., Gildersleeve, J., Kahne, D., Clausen, H., Danishefsky, S. J., and Livingston, P. O. (2005) Comparison of antigen constructs and carrier molecules for augmenting the immunogenicity of the monosaccharide epithelial cancer antigen Tn. *Cancer Immunol. Immunother. 54*, 424−430.
(17) Osinaga, E., Bay, S., Tello, D., Babino, A., Pritsch, O., Assemat, K., Cantacuzene, D., Nakada, H., and Alzari, P. (2000) Analysis of the fine specificity of Tn-binding proteins using synthetic glycopeptide epitopes and a biosensor based on surface plasmon resonance spectroscopy. *FEBS Lett. 469*, 24−28.
(18) Kracun, S. K., Clo, E., Clausen, H., Levery, S. B., Jensen, K. J., and Blixt, O. (2010) Random glycopeptide bead libraries for seromic biomarker discovery. *J. Proteome Res. 9*, 6705−6714.
(19) Blixt, O., Clo, E., Nudelman, A. S., Sorensen, K. K., Clausen, T., Wandall, H. H., Livingston, P. O., Clausen, H., and Jensen, K. J. (2010) A high-throughput O-glycopeptide discovery platform for seromic profiling. *J. Proteome Res. 9*, 5250−5261.
(20) Brooks, C. L., Schietinger, A., Borisova, S. N., Kufer, P., Okon, M., Hirama, T., MacKenzie, C. R., Wang, L. X., Schreiber, H., and Evans, S. V. (2010) Antibody recognition of a unique tumor-specific glycopeptide antigen. *Proc. Natl. Acad. Sci. U.S.A. 107*, 10056−10061.
(21) Takeuchi, H., Kato, K., Hassan, H., Clausen, H., and Irimura, T. (2002) O-GalNAc incorporation into a cluster acceptor site of three consecutive threonines - distinct specificity of GalNAc-transferase isoforms. *Eur. J. Biochem. 269*, 6173−6183.
(22) Liu, M., Barany, G., and Live, D. (2005) Parallel solid-phase synthesis of mucin-like glycopeptides. *Carbohydr. Res. 340*, 2111−2122.
(23) Barb, A. W., Borgert, A. J., Liu, M. A., Barany, G., and Live, D. (2010) Intramolecular glycan-protein interactions in glycoproteins. *Methods Enzymol. 478*, 365−388.
(24) Wang, A. C., and Bax, A. (1996) Determination of the backbone dihedral angles phi in human ubiquitin from reparametrized empirical Karplus equations. *J. Am. Chem. Soc. 118*, 2483−2494.
(25) Schmidt, J. M. (2007) A versatile component-coupling model to account for substituent effects: Application to polypeptide phi and chi 1 torsion related ^{3}J data. *J. Magn. Reson. 186*, 34−50.
(26) Ottiger, M., and Bax, A. (1999) Bicelle-based liquid crystals for NMR-measurement of dipolar couplings at acidic and basic pH values. *J. Biomol. NMR 13*, 187−191.
(27) Schuster, O., Klich, G., Sinnwell, V., Kranz, H., Paulsen, H., and Meyer, B. (1999) 'Wave-type' structure of a synthetic hexaglycosylated decapeptide: A part of the extracellular domain of human glycophorin A. *J. Biomol. NMR 14*, 33−45.
(28) Dziadek, S., Griesinger, C., Kunz, H., and Reinscheid, U. M. (2006) Synthesis and structural model of an alpha(2,6)-sialyl-T glycosylated MUC1 eicosapeptide under physiological conditions. *Chem.—Eur. J. 12*, 4981−4993.
(29) Hashimoto, R., Fujitani, N., Takegawa, Y., Kurogochi, M., Matsushita, T., Naruchi, K., Ohyabu, N., Hinou, H., Gao, X. D., Manri, N., Satake, H., Kaneko, A., Sakamoto, T., and Nishimura, S. I. (2011) An efficient approach for the characterization of mucin-type glycopeptides: The effect of O-glycosylation on the conformation of synthetic mucin peptides. *Chem.—Eur. J. 17*, 2393−2404.
(30) Narimatsu, Y., Kubota, T., Furukawa, S., Morii, H., Narimatsu, H., and Yamasaki, K. (2010) Effect of glycosylation on cis/trans isomerization of prolines in IgA1-hinge peptide. *J. Am. Chem. Soc. 132*, 5548−5549.
(31) Kuhn, B., Mohr, P., and Stahl, M. (2010) Intramolecular hydrogen bonding in medicinal chemistry. *J. Med. Chem. 53*, 2601−2611.
(32) Lo-Man, R., Vichier-Guerre, S., Perraut, R., Deriaud, E., Huteau, V., BenMohamed, L., Diop, O. M., Livingston, P. O., Bay, S., and Leclerc, C. (2004) A fully synthetic therapeutic vaccine candidate targeting carcinoma-associated tn carbohydrate antigen induces tumor-specific antibodies in nonhuman primates. *Cancer Res. 64*, 4987−4994.
(33) Morita, N., Yajima, Y., Asanuma, H., Nakada, H., and Fujita-Yamaguchi, Y. (2009) Inhibition of cancer cell growth by anti-Tn monoclonal antibody MLS128. *Biosci. Trends 3*, 32−37.
(34) Blixt, O., Head, S., Mondala, T., Scanlan, C., Huflejt, M. E., Alvarez, R., Bryan, M. C., Fazio, F., Calarese, D., Stevens, J., Razi, N., Stevens, D. J., Skehel, J. J., van Die, I., Burton, D. R., Wilson, I. A., Cummings, R., Bovin, N., Wong, C. H., and Paulson, J. C. (2004) Printed covalent glycan array for ligand profiling of diverse glycan binding proteins. *Proc. Natl. Acad. Sci. U.S.A. 101*, 17033−17038.
(35) Oyelaran, O., and Gildersleeve, J. C. (2009) Glycan arrays: Recent advances and future challenges. *Curr. Opin. Chem. Biol. 13*, 406−413.
(36) Smith, D. F., Song, X. Z., and Cummings, R. D. (2010) Use of glycan microarrays to explore specificity of glycan-binding proteins. *Methods Enzymol. 480*, 417−444.
(37) Godula, K., Rabuka, D., Nam, K. T., and Bertozzi, C. R. (2009) Synthesis and microcontact printing of dual end-functionalized mucin-like glycopolymers for microarray applications. *Angew. Chem., Int. Ed. 48*, 4973−4976.
(38) Gestwicki, J. E., Cairo, C. W., Mann, D. A., Owen, R. M., and Kiessling, L. L. (2002) Selective immobilization of multivalent ligands for surface plasmon resonance and fluorescence microscopy. *Anal. Biochem. 305*, 149−155.
(39) Oyelaran, O., Li, Q., Farnsworth, D., and Gildersleeve, J. C. (2009) Microarrays with varying carbohydrate density reveal distinct subpopulations of serum antibodies. *J. Proteome Res. 8*, 3529−3538.
(40) Li, Q. A., Rodriguez, L. G., Farnsworth, D. F., and Gildersleeve, J. C. (2011) Effects of hapten density on the induced antibody repertoire. *ChemBioChem 11*, 1686−1691.
(41) Fritz, T. A., Raman, J., and Tabak, L. A. (2006) Dynamic association between the catalytic and lectin domains of human UDP-GalNAc:

Polypeptide alpha-N-acetylgalactosaminyltransferase-2. *J. Biol. Chem. 281*, 8613−8619.
(42) Bolscher, J. G. M., Brevoord, J., Nazmi, K., Ju, T. Z., Veerman, E. C. I., van Wijk, J. A. E., Cummings, R. D., and van Die, I. (2010) Solid-phase synthesis of a pentavalent GalNAc-containing glycopeptide (Tn antigen) representing the nephropathy-associated IgA hinge region. *Carbohydr. Res. 345*, 1998−2003.
(43) Babino, A., Tello, D., Rojas, A., Bay, S., Osinaga, E., and Alzari, P. M. (2003) The crystal structure of a plant lectin in complex with the Tn antigen. *FEBS Lett. 536*, 106−110.
(44) Sanchez, J. F., Lescar, J., Chazalet, V., Audfray, A., Gagnon, J., Alvarez, R., Breton, C., Imberty, A., and Mitchell, E. P. (2006) Biochemical and structural analysis of helix pomatia agglutinin - a hexameric lectin with a novel fold. *J. Biol. Chem. 281*, 20171−20180.
(45) Avichezer, D., Springer, G. F., Schechter, B., and Arnon, R. (1997) Immunoreactivities of polyclonal and monoclonal anti-T and anti-Tn antibodies with human carcinoma cells, grown in vitro and in a xenograft model. *Int. J. Cancer 72*, 119−127.
(46) Springer, G. F., Chandrasekaran, E. V., Desai, P. R., and Tegtmeyer, H. (1988) Blood-group Tn-active macromolecules from human carcinomas and erythrocytes - characterization of and specific reactivity with monoclonal and polyclonal anti-Tn antibodies induced by various immunogens. *Carbohydr. Res. 178*, 271−292.
(47) Manimala, J. C., Roach, T. A., Li, Z., and Gildersleeve, J. C. (2007) High-throughput carbohydrate microarray profiling of 27 antibodies demonstrates widespread specificity problems. *Glycobiology 17*, 17C−23C.
(48) Liu, M. A., Borgert, A., Barany, G., and Live, D. (2008) Conformational consequences of protein glycosylation: Preparation of O-mannosyl serine and threonine building blocks, and their incorporation into glycopeptide sequences derived from alpha-dystroglycan. *Biopolymers 90*, 358−368.
(49) van de Ven, F. J. M. (1995) *Multidimensional NMR in Liquids*, Wiley-VCH, New York.
(50) Schwieters, C. D., Kuszewski, J. J., and Clore, G. M. (2006) Using Xplor-NIH for NMR molecular structure determination. *Prog. Nucl. Magn. Reson. Spectrosc. 48*, 47−62.
(51) Gilewski, T., Adluri, S., Ragupathi, G., Zhang, S. L., Yao, T. J., Panageas, K., Moynahan, M., Houghton, A., Norton, L., and Livingston, P. O. (2000) Vaccination of high-risk breast cancer patients with mucin-1 (MUC1) keyhole limpet hemocyanin conjugate plus QS-21. *Clin. Cancer. Res. 6*, 1693−1701.
(52) Tarp, M. A., Sorensen, A. L., Mandel, U., Paulsen, H., Burchell, J., Taylor-Papadimitriou, J., and Clausen, H. (2007) Identification of a novel cancer-specific immunodominant glycopeptide epitope in the MUC1 tandem repeat. *Glycobiology 17*, 197−209.